

Epigenetic Modulation of Collagen 1A1: Therapeutic Implications in Fibrosis and Endometriosis 1

Authors: Zheng, Ye, Khan, Zaraq, Zanfagnin, Valentina, Correa, Luiz F., Delaney, Abigail A., et al.

Source: Biology of Reproduction, 94(4)

Published By: Society for the Study of Reproduction

URL: <https://doi.org/10.1095/biolreprod.115.138115>

BioOne Complete (complete.BioOne.org) is a full-text database of 200 subscribed and open-access titles in the biological, ecological, and environmental sciences published by nonprofit societies, associations, museums, institutions, and presses.

Your use of this PDF, the BioOne Complete website, and all posted and associated content indicates your acceptance of BioOne's Terms of Use, available at www.bioone.org/terms-of-use.

Usage of BioOne Complete content is strictly limited to personal, educational, and non - commercial use. Commercial inquiries or rights and permissions requests should be directed to the individual publisher as copyright holder.

BioOne sees sustainable scholarly publishing as an inherently collaborative enterprise connecting authors, nonprofit publishers, academic institutions, research libraries, and research funders in the common goal of maximizing access to critical research.

Epigenetic Modulation of Collagen 1A1: Therapeutic Implications in Fibrosis and Endometriosis¹

Ye Zheng, Zaraq Khan, Valentina Zanfagnin, Luiz F. Correa, Abigail A. Delaney, and Gaurang S. Daftary²

Laboratory of Translation Epigenetics in Reproduction, Department of Obstetrics and Gynecology, Mayo Clinic, Rochester, Minnesota

ABSTRACT

Progressive fibrosis is recalcitrant to conventional therapy and commonly complicates chronic diseases and surgical healing. We evaluate here a novel mechanism that regulates scar-tissue collagen (COL1A1/Col1a1) expression and characterizes its translational relevance as a targeted therapy for fibrosis in an endometriosis disease model. Endometriosis is caused by displacement and implantation of uterine endometrium onto abdominal organs and spreads with progressive scarring. Transcription factor KLF11 is specifically diminished in endometriosis lesions. Loss of KLF11-mediated repression of COL1A1/Col1a1 expression resulted in increased fibrosis. To determine the biological significance of COL1A1/Col1a1 expression on fibrosis, we modulated its expression. In human endometrial-stromal fibroblasts, KLF11 recruited SIN3A/HDAC (histone deacetylase), resulting in COL1A1-promoter deacetylation and repression. This role of KLF11 was pharmacologically replicated by a histone acetyl transferase inhibitor (garcinol). In contrast, opposite effects were obtained with a HDAC inhibitor (suberoyl anilide hydroxamic acid), confirming regulatory specificity for these reciprocally active epigenetic mechanisms. Fibrosis was concordantly reversed in *Klf11*^{−/−} animals by histone acetyl transferase inhibitor and in wild-type animals by HDAC inhibitor treatments. Aberrant lesional COL1A1 regulation is significant because fibrosis depended on lesion rather than host genotype. This is the first report demonstrating feasibility for targeted pharmacological reversal of fibrosis, an intractable phenotype of diverse chronic diseases.

collagen 1, endometriosis, epigenetic modulators, fibrosis, gene transcription

INTRODUCTION

Fibrosis is critical for wound healing; however, when dysregulated, it becomes prolific and symptomatic from loss of functional organ tissue, resulting in diseases such as cirrhosis, Crohn's disease, and pulmonary fibrosis [1–3]. Fibrosis also prominently affects connective tissues in multisystem chronic

and autoimmune diseases such as fibromyalgia and scleroderma as well as complicates postsurgical healing [4, 5]. Additionally, fibrosis occurs as part of epithelial-mesenchymal transition in a variety of cancers wherein it is associated with adverse prognosis [6]. We have used an endometriosis disease model to investigate chronic systemic fibrosis.

Endometriosis is a common disease that affects 10% of women and causes chronic morbidity from pain, infertility, and sexual and pelvic dysfunction [7]. The disease is characterized by implants of endometrial epithelial and stromal cells in ectopic locations outside the uterine cavity. The lesions are associated with proliferic fibrosis that entraps abdominal and pelvic organs into a highly distorted frozen pelvis with concomitant multi-organ functional impairment [8]. The extent of fibrosis influences disease staging as well as morbidity [9]. Fibrosis is also a highly recalcitrant disease phenotype linked to morbidity and recurrence after conventional surgical treatment for the disease [10]. Endometriosis is an excellent disease model for mechanistic and translation investigation of chronic fibrosis and scarring due to its high prevalence, natural history of prominent scarring, and frequent coexistence with other chronic fibrotic diseases [11, 12].

Sp/KLF transcription factors regulate most expressed genes by binding ubiquitous, genomic GC-rich regulatory elements [13]. Differences in tissue expression levels and/or GC-rich element-binding preferences contribute to regulatory specificity amongst family members. KLF11 is highly expressed in endocrine-regulated and developmentally related urogenital tissues, wherein it is significantly associated with common human diseases such as leiomyoma, endometriosis, and diabetes [14, 15]. In humans, KLF11 is selectively diminished in endometriosis lesions; loss of Klf11 regulation is associated with disease progression and fibrosis in an animal model [16]. KLF11/Klf11 therefore has a role in fibrotic progression with relevance to human disease. We have mechanistically investigated the regulation of the predominant scar tissue protein COL1A1/Col1a1 in vitro by KLF11 and further characterized the translational relevance of this regulatory mechanism in vivo in an animal model [16, 17].

MATERIALS AND METHODS

Ethics Statement

All animal experiments were performed as outlined in a study protocol approved by the Institutional Animal Care and Use Committee at Mayo Clinic, Rochester, MN.

Experimental Animals

C57/BL6 wild-type (wt) and *Klf11*^{−/−} mice (8-wk old) were used. Endometriosis was induced using a published surgical approach [16]. Two 5-mm everted uterine segments were transplanted by suture to the flank parietal peritoneum, one implant per side. All animals were in estrus phase at induction. In allograft transplant experiments (Fig. 1), *Klf11*^{−/−} uterine segments were allografted into wt peritoneal cavities and vice versa (n = 16; two groups: eight

¹Supported by Mayo Clinic Institutional Funds and Fraternal Order of Eagles Pilot Award.

²Correspondence: Gaurang S. Daftary, Laboratory of Translation Epigenetics in Reproduction, Department of Obstetrics and Gynecology, Mayo Clinic, 200 First Street SW, Rochester, MN 55905. E-mail: daftary.gaurang@mayo.edu

Received: 21 December 2015.

First decision: 22 January 2016.

Accepted: 25 February 2016.

© 2016 by the Society for the Study of Reproduction, Inc. This is an Open Access article, freely available through Biology of Reproduction's Authors' Choice option, and is available under a Creative Commons License 4.0 (Attribution-Non-Commercial), as described at <http://creativecommons.org/licenses/by-nc/4.0>

eISSN: 1529-7268 <http://www.biolreprod.org>

ISSN: 0006-3363

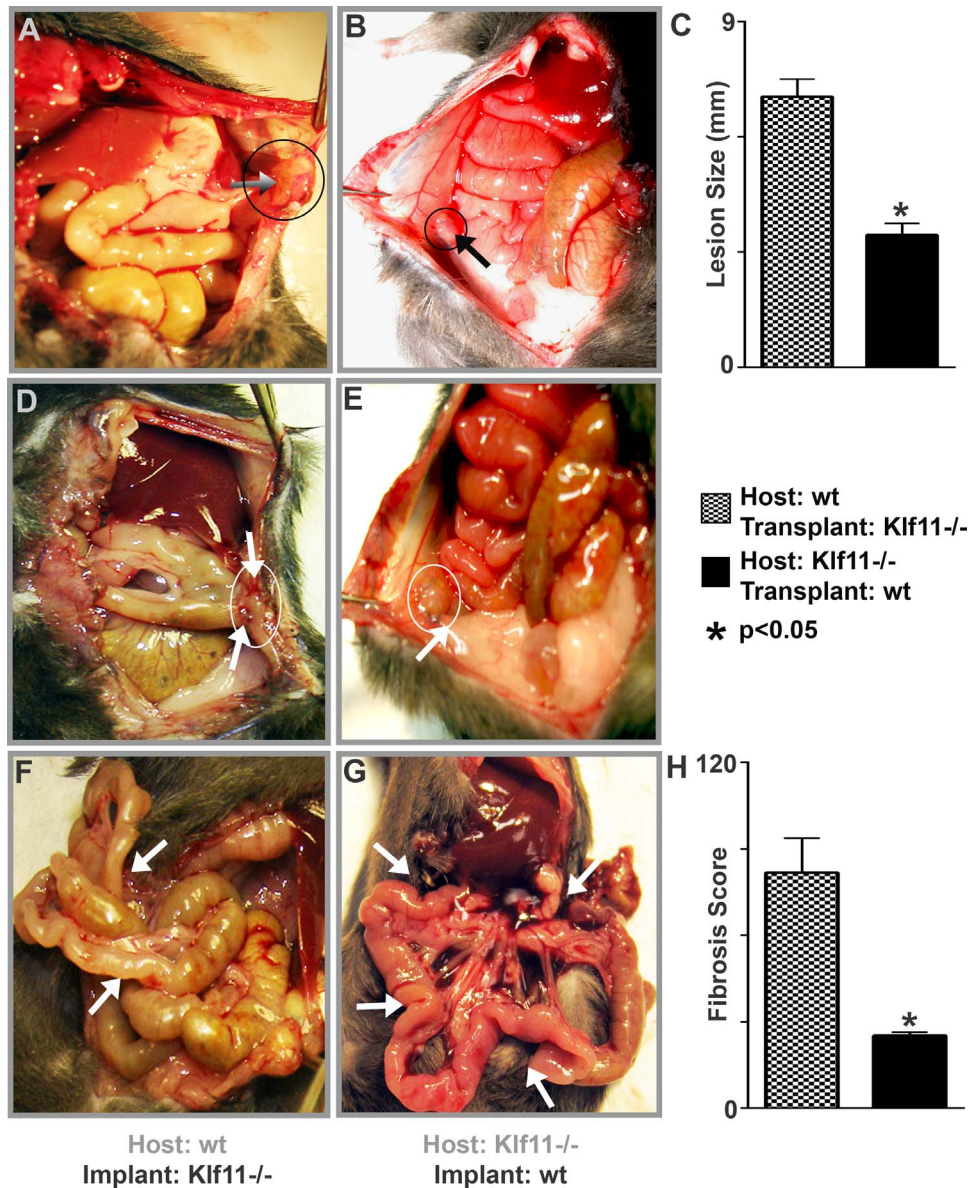


FIG. 1. Disease progression is associated with implant rather than host genotype. Uterine segments (0.5 cm) were allografted from 8-wk-old Klf11^{-/-} to wt female mice and vice versa and evaluated 3 wk postinduction (n = 8/group). **A, B** Klf11^{-/-} lesions transplanted in wt animals were larger (**A**) compared to wt lesions in Klf11^{-/-} animals (**B**). Representative lesions shown (encircled and arrows). **C** Mean lesion size of Klf11^{-/-} lesions (in wt) and wt lesions (in Klf11^{-/-}) were 6.3 ± 0.4 mm versus 3.2 ± 0.3 mm, respectively (* $P < 0.05$). **D, E** Dense adhesions in wt animals with Klf11^{-/-} lesions obliterated tissue planes. In contrast, adhesions in Klf11^{-/-} animals with wt lesions were discrete and flimsy. Representative lesions shown (**D, E**: ellipse, lesion; arrow, adhesion). **F, G** Klf11^{-/-} implants in wt animals were associated with mesenteric fibrosis (**F**, arrows). In contrast, no mesenteric scarring was observed in Klf11^{-/-} animals with wt lesions (**G**, arrows). **H** Fibrosis scores of 87 ± 4.2 and 28 ± 0.44 were associated with Klf11^{-/-} lesions in wt hosts and wt lesions in Klf11^{-/-} hosts, respectively (* $P < 0.05$, implant Klf11^{-/-}/host wt compared to implant wt/host Klf11^{-/-}).

wt recipients of Klf11^{-/-} uterine segments and eight Klf11^{-/-} recipients of wt uterine segments).

For experiments involving epigenetic inhibitor treatments and corresponding controls (see Figs. 4 and 5), endometriosis implants were autologous; two 5-mm uterine segments from each animal were sutured to its parietal peritoneum, one implant per side, at the time of surgical induction of lesions. The animals were then treated postoperatively with 1) 0.2 μ g/g garcinol (Enzo), a histone acetyl transferase inhibitor (HATI), 2) 50 μ g/g suberoyl anilide hydroxamic acid (SAHA) (Cayman), a histone deacetylase inhibitor (HDACI), or 3) (v/v) dimethyl sulfoxide (DMSO) by intraperitoneal injection daily for 3 wk (n = 60; six groups of 10 animals each: wt: treated with DMSO, HATI, or SAHA and Klf11^{-/-} treated with DMSO, HATI, or SAHA). Treatment regimens were based on dose-optimization and published studies to ensure nontoxic, therapeutic efficacy. Evaluation at necropsy was done 3 wk postinduction.

Human Endometrial Stromal Cell Culture and Treatments

Human endometrial-stromal cells (T-HESCs) are extensively characterized and were purchased from ATCC (CRL-4003), evaluated for contamination, and maintained in Dulbecco-modified Eagle medium containing 10% fetal bovine serum [18]. Stable cell lines expressing empty vector (EV, i.e., pcDNA3/His), KLF11 (pcDNA3/His-KLF11) or KLF11EAPP (pcDNA3/His/KLF11EAPP) were established using the pCDH-EF1-IRES-CopGFP lentiviral vector (System Biosciences). Cells were treated with 15 μ M garcinol (i.e., a HATI), 4 μ M SAHA (i.e., an HDACI), or (v/v) DMSO (Sigma) for 48 h as previously described [19].

RNA Isolation and Real-time PCR

Standard protocols were used for RNA isolation and PCR as described previously [19]. Two micrograms of RNA was used for analysis. For cDNA

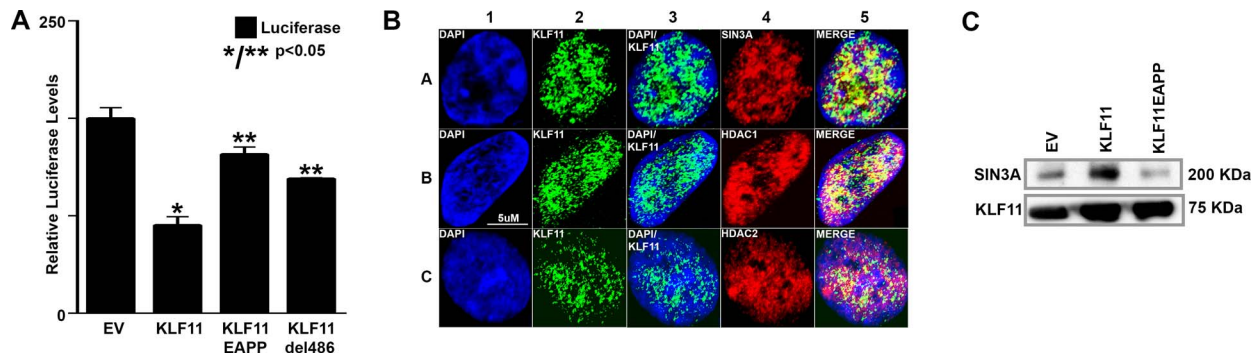


FIG. 2. KLF11 repressed COL1A1 in T-HESCs via the epigenetic SIN3/HDAC mechanism. **A**) T-HESCs were cotransfected with pcDNA3/*HIS* (EV), pcDNA3/*HIS-KLF11*, pcDNA3/*HIS-KLF11EAPP*, or pcDNA3/*HIS-KLF11del486* and a pGL3/*COL1A1*-promoter-reporter construct. KLF11 repressed *COL1A1*-luciferase activity 2-fold compared to EV (100 ± 5.5 vs. 45.2 ± 4.2 , respectively, $*P < 0.05$). In contrast, KLF11EAPP and KLF11del486 derepressed *COL1A1* promoter luciferase (81.6 ± 3.6 and 69 ± 0.4 , respectively, $**P < 0.05$ compared to EV and KLF11). Luciferase levels were normalized to total lysate protein concentration. Assays were repeated in triplicate three times. **B**) Representative images show co-immunolocalization of KLF11, SIN3A, HDAC1, and HDAC2 in T-HESC nuclei. 4',6-Diamidino-2-phenylindole dihydrochloride staining revealed blue heterochromatin and dark euchromatin domains (column 1, rows A–C). KLF11 (green: column 3, rows A–C) and SIN3A, HDAC1, and HDAC2 (red: column 4, rows A, B, and C, respectively) localized predominantly to euchromatin (column 5: merge, rows A–C). Magnification $\times 800$. **C**) KLF11 binding to SIN3A was confirmed in EV, *HIS-KLF11*, or *HIS-KLF11EAPP* transfected T-HESCs. Immunoprecipitation was by anti-KLF11 and detection with anti-SIN3A (upper panel). The blot was reprobed with anti-KLF11 to detect protein loading (lower panel). Transfected KLF11 (KLF11) bound SIN3A much more avidly compared to endogenous KLF11 in EV-transfected cells. In KLF11EAPP-transfected cells, only endogenous KLF11 bound SIN3A. The lower panel reveals differences in immunoprecipitated KLF11 levels in transfected T-HESCs.

synthesis, oligo-dT primer was used in the Superscript III first-strand system (Invitrogen). Real-time PCR was performed using commercial primers for *COL1A1* (Qiagen) and a panel of housekeeping controls: glyceraldehyde-3-phosphate dehydrogenase (*GAPDH/Gapdh*), beta-2-microglobulin (*B2M/B2m*), and hypoxanthine phosphoribosyltransferase 1 (*HPRT1/Hprt1*) (Qiagen). PCR optimization and controls were performed as described previously [16, 19, 20]. Quantitative PCR reactions were performed using the IQ-SYBR Green Supermix (Bio-Rad) in a PikoReal96 Real-Time PCR System (Thermo-Scientific). Each experiment was done in triplicate three independent times.

Immunohistochemistry, Immunofluorescence, and Tissue Microarray Design

Tissue microarrays of 28 patients made up of eutopic endometrium and endometriosis tissues from the same individual was created from Mayo Clinic Pathology archives and used as described [16]. The tissue microarray was generated per a protocol approved by the Mayo Clinic Institutional Review Board. Standard published laboratory protocols for immunohistochemistry and immunofluorescence were followed [16, 19, 21]. The following antibodies were used for immunofluorescence: rabbit anti-KLF11 (1:1000, H00008462-M01; Abnova) and a fluorescein isothiocyanate/Alexa Fluor 488-conjugated anti-rabbit secondary antibody (1:500; Invitrogen). For SIN3A, HDAC1, and HDAC2, mouse anti-SIN3A, HDAC1, and HDAC2 (1:500, sc-994, sc-81598, and sc-7899, respectively; Santa Cruz Biotechnology) were used with a rhodamine/Alexa Fluor 555-conjugated anti-mouse secondary antibody (1:250; Invitrogen). DNA was stained with 4',6-diamidino-2-phenylindole dihydrochloride (Vector Labs). Fluorescence was observed using an argon-krypton laser on a Zeiss LSM-510 confocal microscope. For immunohistochemistry, anti-KLF11 (clone 8F4; 1:100 dilution; Abnova) was used with overnight incubation at 4°C as previously described [16]. Histochemical staining for collagen deposition using Masson trichrome was performed by the Mayo Pathology Department Core Laboratory.

Chromatin Immunoprecipitation

Chromatin immunoprecipitation (ChIP) was performed using E-Z ChIP per kit protocol (Millipore) as described [16, 19–21]. Briefly, 2×10^6 cells were lysed and sonicated to generate 200 ~ 600 bp fragments. Anti-acetyl histone 3K9 antibody (1:250, ab4441; Abcam), or a species-specific control immunoglobulin G (IgG) (171870; Abcam) was used for overnight immunoprecipitation. KLF11-binding promoter elements were evaluated for differences in histone acetylation. Human *COL1A1* (–785 to –433) was amplified using forward primer CCACCTAGTCATGTTTCTC and reverse primer CTGGCAAGAGCTAAGGGA; mouse *Col1a1* (–600 to –400) was amplified using forward primer GGCACCCCCTTCCTTTCAAC and reverse primer GTAATCTTTCAGGCATCCTGGGG. PCR products were examined on a 2% agarose gel. Four hundred milligrams frozen mouse uterus implant

tissue from necropsy was used for ChIP assay using a ChIP-IT High Sensitivity kit (Activemotif) following the manufacturer's protocol. The tissue was minced and fixed in 10% formaldehyde for 15 min on ice, and then homogenized, lysed, and sonicated to generate 200 to ~600 bp chromatin DNA fragments. Sixty micrograms sheared chromatin DNA from each sample was used for ChIP with 4 μ g anti-AcH3K9 or a species-specific control IgG as negative control.

Western Blot Analysis and Co-immunoprecipitation

Whole-cell lysate was obtained from transduced T-HESCs expressing KLF11, KLF11EAPP, or EV. The lysate was incubated overnight at 4°C with anti-KLF11 (1:200, H00008462; Abnova) or anti-SIN3A (1:200, sc-994; Santa Cruz) antibody followed by a 2-h incubation with protein G agarose beads (Millipore). Immunoprecipitate collected after washing and elution was analyzed by Western blots using anti-KLF11 (1:500, H00008462-M01; Abnova) and anti-SIN3A (1:500, sc-994; Santa Cruz Biotechnology) primary antibodies [19]. Quantification of Western blots was performed using Image-J software (National Institutes of Health).

Luciferase Reporter Assay

The pGL3-basic empty vector was purchased from Promega. Promoter-reporter constructs containing serial 200–400 bp GC-rich elements in the *COL1A1* promoter were generated as previously described [16]. Eighty percent confluent T-HESCs were cotransfected with 2.5 μ g pcDNA3/His (EV) (Invitrogen), pcDNA3/*HIS-KLF11*, pcDNA3/*HIS-KLF11EAPP*, or pcDNA3/*HIS-KLF11del486* constructs and 3 μ g pGL3 *COL1A1*-promoter-reporter construct (–785 to –433; ChIP-validated region). Reporter activity was determined 48 h posttransfection using the Luciferase assay system (Promega) and a 20/20 luminometer per the manufacturer's protocol. Data in relative light units was normalized to lysate protein concentrations as characterized previously [21]. Experiments were performed in triplicate, three independent times.

Statistical Analysis

All calculations were performed with biostatistician input. Animal numbers were based on 80% power to determine an effect-size of at least 30% difference in lesion measurement and fibrosis scores with a type I error of 0.05 using two-tailed tests [9, 16, 22]. Results were evaluated and scored independently by at least three authors blinded to genotype and treatment condition. All results are expressed as means \pm standard error of means (SEM). In vitro experiments were performed on at least three independent biological replicates. The Bonferroni method (*t* tests) or chi-square tests were used per data type. All statistical tests were two-sided. Statistical analysis was performed using SAS

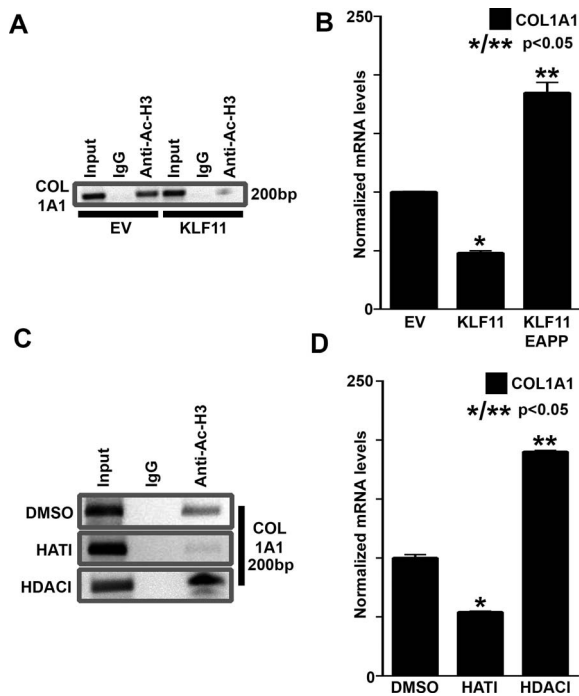


FIG. 3. COL1A1 expression was regulated via promoter histone deacetylation. **A**) Histone deacetylation was detected using anti-acetyl histone H3K9 (Anti-Ac-H3) in T-HESCs transduced with pcDNA3/HIS (EV) or pcDNA3/HIS-KLF11. Diminished binding in KLF11-transfected cells compared to EV suggested deacetylation. No binding was detected in controls using a species- and isotype-specific antibody (IgG); representative result shown. **B**) Increased COL1A1 mRNA expression was seen in KLF11EAPP-transduced T-HESCs compared to wtKLF11 or EV (184.89 ± 8.8 vs. 48.11 ± 1.87 and 100 ± 0.43 , respectively; $*P < 0.05$ compared to EV; $**P < 0.05$ compared to EV and KLF11). Messenger RNA levels were normalized to HPRT1, GAPDH, and B2M. Results represent three replicates. **C**) T-HESCs were treated with 15 μ M HAT1 or 4 μ M HDACI. Acetylated H3K9 levels were highest in HDACI-treated cells, intermediate in vehicle (DMSO)-treated cells, and least in HAT1-treated cells. No binding was detected with a species- and isotype-specific antibody (IgG); Representative result shown. **D**) COL1A1 mRNA expression was activated by HDACI (190 ± 1.1) and repressed by HAT1 (54 ± 0.77) compared to vehicle (DMSO)-treated cells (100 ± 2.81 ; $*P < 0.05$ compared to DMSO; $**P < 0.05$ compared to DMSO and HAT1 treatments). Messenger RNA levels were normalized to HPRT1, GAPDH, and B2M. Results represent five replicates.

software (SAS Institute). For consistency, all P values are reported as < 0.05 throughout, where significant.

RESULTS

Disease Progression Is Associated with Implant Rather Than Host Genotype

Endometriosis is characterized by diminished KLF11 expression in human disease lesions compared to corresponding normal uterine endometrium [16]. To differentiate between fibrosis due to lesional loss of Klf11 regulation as seen in human disease from generalized loss as in the Klf11^{-/-} mouse disease model, we transplanted uterine fragments from Klf11^{-/-} mice into age-matched wt animals and vice versa.

Larger lesions and prolific fibrosis typically seen in Klf11^{-/-} animals were observed in wt animals that received Klf11^{-/-} uterine implants (Fig. 1, A, C, and D). The intensity and extent of fibrosis mirrored human disease. Spreading fibrosis involved the intestinal mesentery; as a result, the intestines could not be anatomically delineated by unraveling

(Fig. 1F). Fibrotic extent was visually quantified based on a weighted adhesion scoring system as in human disease that was adapted for murine anatomy [9, 16, 22]. Adhesion scores in wt animals with Klf11^{-/-} implants indicated rapid disease progression (Fig. 1H).

In contrast, Klf11^{-/-} mice that received wt implants had small lesions with diminished fibrotic progression as previously seen in wt animals (Fig. 1, B, C, and E). These animals also did not display mesenteric scarring (Fig. 1G) and had low fibrosis progression scores (Fig. 1H). Lesional Col1a1 mRNA and protein expression were selectively elevated only in Klf11^{-/-} implants, which correlated directly with increased fibrosis associated with such lesions (Supplemental Fig. S1; Supplemental Data are available online at www.biolreprod.org). The data from these allograft experiments suggests that lesion-specific diminished Klf11 levels and transcriptional dysregulation of Col1a1 were critical for disease progression.

KLF11 Repressed COL1A1 via the Epigenetic SIN3A/HDAC Mechanism in T-HESCs

We have previously characterized promoter binding and repression of COL1A1 by KLF11. KLF11 recruits and binds the epigenetic corepressors SIN3A/HDAC and heterochromatin protein 1 (HP1) to repress target genes [19, 20, 23]. To determine if these mechanisms mediate repression of COL1A1 by KLF11 in T-HESCs, we used mutagenized constructs KLF11EAPP and KLF11del486 that specifically do not bind SIN3A/HDAC and HP1 respectively [24, 25]. Whereas KLF11 repressed COL1A1-promoter-luciferase activity compared to EV, both mutagenized constructs derepressed the promoter (Fig. 2A). This suggests that derepression of the COL1A1 promoter was a result of nonrecruitment of respective epigenetic corepressors by mutagenized KLF11. The SIN3A corepressor complex causes HDAC-mediated promoter histone deacetylation near the transcription factor binding site, resulting in chromatin compaction and transcriptional repression [20, 26]. In contrast, acetylation of promoter histones causes chromatin to expand, which is permissive to transcription.

We further determined endogenous expression of KLF11, SIN3A, and HDAC1 and 2 in T-HESCs; KLF11 colocalized with SIN3A, while HDAC1 and 2 localized to euchromatic nuclear domains (Fig. 2B). This suggests that in T-HESCs, KLF11/SIN3A/HDAC regulated actively transcribed euchromatic genes. In addition to colocalization, SIN3A/HDAC bound to KLF11 but not to the KLF11EAPP mutant in T-HESCs (Fig. 2C). KLF11 therefore interacted with SIN3A via its N-terminal in T-HESCs.

COL1A1 Expression in T-HESCs Was Regulated via Promoter Histone Deacetylation

To determine if SIN3A/HDAC recruitment by KLF11 resulted in COL1A1 promoter histone deacetylation in the vicinity of the KLF11-binding element, we evaluated this region by ChIP using an anti-acetyl histone antibody. In contrast to EV-transduced controls, promoter acetylation was decreased in KLF11-transduced cells consequent to KLF11/SIN3A/HDAC-mediated histone deacetylation (Fig. 3A). KLF11/SIN3A/HDAC also repressed COL1A1 mRNA expression concordant with a promoter effect (Fig. 3B). Our data thus suggests that KLF11 recruits SIN3A/HDAC to the COL1A1 promoter, wherein localized histone deacetylation results in repression.

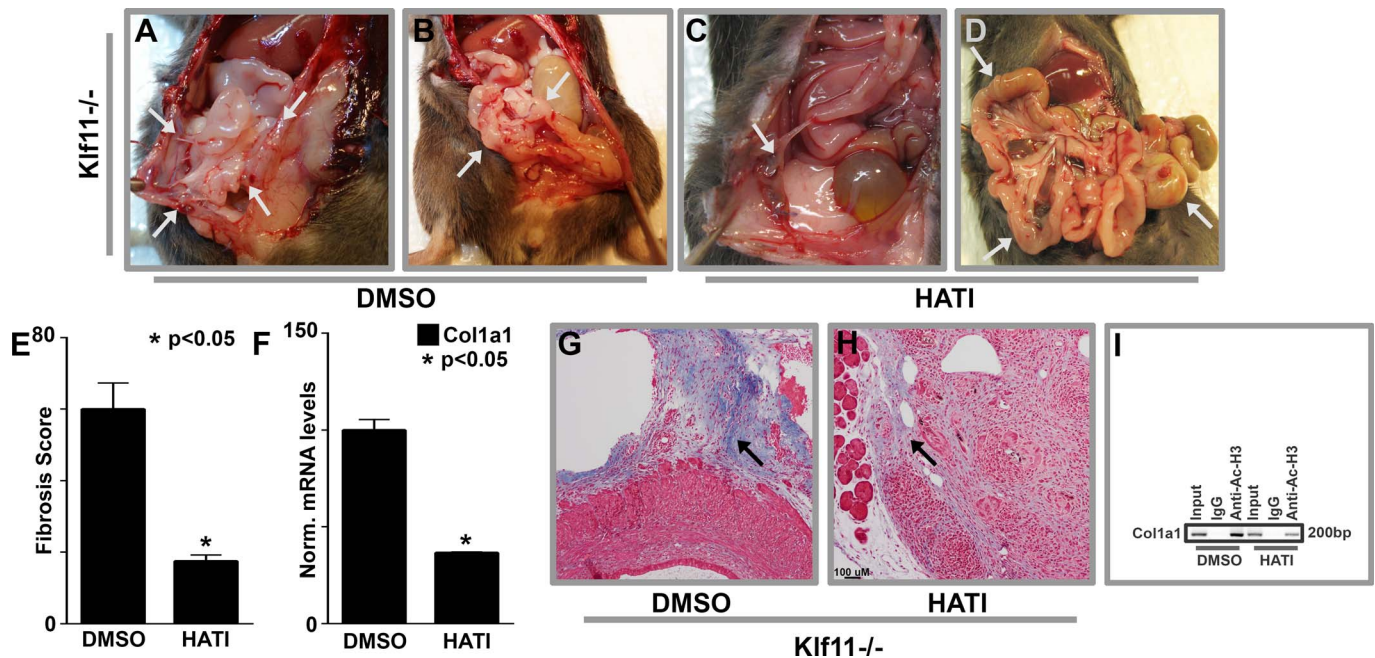


FIG. 4. HATI treatment in *Klf11*^{-/-} mice reverses fibrotic progression. **A, B** Vehicle (DMSO)-treated *Klf11*^{-/-} animals developed dense fibrosis (**A**, arrows) and mesenteric involvement with inability to unravel the intestines (**B**, arrows). Representative results shown (n = 10). **C, D** HATI-treated *Klf11*^{-/-} animals had discrete, flimsy adhesions (**C**, arrow) with minimal mesenteric fibrosis (**D**, arrows). Representative results shown (n = 10). **E** Fibrosis scores were diminished in HATI- compared to DMSO-treated *Klf11*^{-/-} animals (17 ± 1.7 vs. 60 ± 7.3 respectively, *P < 0.05; n = 10/group). **F** Lesional *Col1a1* mRNA expression was increased in vehicle compared to HATI-treated *Klf11*^{-/-} animals (100 ± 5.5 vs. 36 ± 0.34, *P < 0.05). Results represent normalized mean *Col1a1* mRNA levels from five lesions/treatment group. **G, H** Col1 levels in perilesional tissues correlated with corresponding mRNA expression levels in DMSO- and HATI-treated *Klf11*^{-/-} animals (**G, H**: blue stain [Masson Trichrome], arrow). Representative lesions shown (n = 10/treatment group; magnification ×400). **I** Col1a1 promoter was relatively deacetylated in HATI compared to DMSO treated *Klf11*^{-/-} animals (decreased band intensity in HATI compared to DMSO). Antibody-binding specificity was confirmed using a species-specific IgG. Representative findings shown (n = 5/treatment group; 1 lesion/animal).

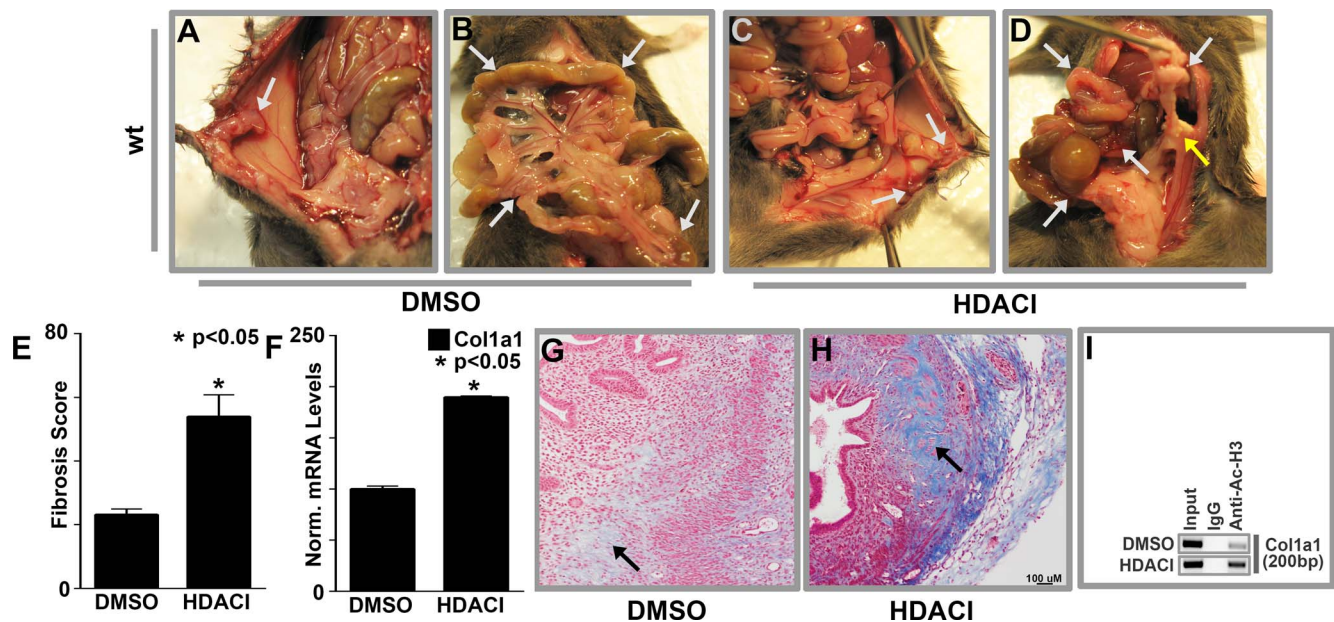


FIG. 5. HDACI treatment in wt mice augmented fibrotic progression. **A, B** Lesions regressed with minimal perilesional adhesions in vehicle (DMSO)-treated wt animals (**A**, arrow) and display of intestinal anatomy (**B**, arrows). Representative results shown (n = 10). **C, D** HDACI-treated wt animals developed dense, spreading fibrosis resulting in loss of anatomic planes (**C**, arrows; **D**, yellow arrow) including the intestinal mesentery (**D**, white arrows). Representative results shown (n = 10). **E** The fibrosis score was significantly increased in wt HDACI- compared to DMSO-treated animals (54 ± 6.84 vs. 23 ± 1.72, *P < 0.05; n = 10 mice/group). **F** Lesional *Col1a1* mRNA expression from HDACI-treated wt animals was significantly increased compared to vehicle-treated controls (190 ± 1.1 vs. 100 ± 2.8, *P < 0.05). Results represent normalized mean *Col1a1* RNA levels from five independent animal lesions/group. **G, H** Differences in *Col1a1* mRNA expression in DMSO- and HDACI-treated animals were congruent with corresponding differences in perilesional Col1a1 expression (blue stain [Masson Trichrome], arrow). Representative lesions shown (n = 10/group; magnification ×400). **I** Compared to DMSO (vehicle)-treated animals, the Col1a1 promoter was relatively hyperacetylated in HDACI-treated wt animals (HDACI compared to DMSO). Antibody binding specificity was confirmed using a species-specific IgG. Representative findings shown (n = 5/group; 1 lesion/animal).

Garcinol (i.e., a HATI) pharmacologically mimics the biological role of KLF11/SIN3A/HDAC by blocking histone acetylation mediated by HATs. Loss of acetyl transferase activity enables unfettered HDAC action, effectively resulting in promoter deacetylation. We thus treated T-HESCs with HATI or vehicle (DMSO). Lower levels of histone acetylation and gene repression were evident in HATI-treated cells in contrast to DMSO-treated cells, (Fig. 3, C and D).

In contrast to HATI, SAHA (i.e., an HDACI) blocks histone deacetylase action, resulting in target-promoter hyperacetylation from sustained HAT activity. We thus treated T-HESCs with SAHA or vehicle (DMSO). In contrast to HATI- or vehicle-treated cells, HDACI treatment resulted in COL1A1 promoter hyperacetylation and increased gene expression (Fig. 3, C and D). We thus found that the reciprocal mechanisms of promoter histone deacetylation/acetylation altered COL1A1 expression and could be pharmacologically targeted.

HATI Treatment in Klf11^{-/-} Mice Reverses Fibrotic Progression

Colla1 expression directly correlated with the extent of fibrosis in our in vivo animal endometriosis model. To determine if transcriptional modulation of Colla1 could alter the extent of fibrosis, we surgically implanted autologous uterine implants to induce endometriosis in Klf11^{-/-} mice and treated them with a HATI. Loss of KLF11/SIN3A/HDAC repression activated COL1A1 expression, which correlated with dense, prolific fibrosis observed in DMSO (vehicle)-treated Klf11^{-/-} animals (Fig. 4A, white arrows). As in human endometriosis, fibrosis was prolific and extended beyond the lesion to involve intra-abdominal viscera such as the intestines, mesentery, and liver. Mesenteric fibrosis resulted in relative shortening of intestinal length and inability to unravel the small and large intestines (Fig. 4B, white arrows). Repression of Colla1 was manifest phenotypically in HATI-treated Klf11^{-/-} animals by significantly diminished fibrosis with scar tissue restricted to the immediate perilesional region. These animals had either none or only discrete, flimsy adhesions to adjacent connective tissue that could be easily severed by mechanical pressure (Fig. 4C, white arrow). There was also minimal fibrotic spread beyond the vicinity of the lesion into the mesentery (Fig. 4D, arrows). Diminished fibrotic density and extent were further reflected by their significantly diminished fibrosis scores compared to vehicle-treated animals (Fig. 4E).

The animals did not display signs of drug toxicity, and their weight remained unchanged across treatment groups over the study duration (Supplemental Fig. S2). To determine if HATI affected Colla1 expression, we evaluated lesional mRNA and protein levels. Colla1 mRNA and protein were significantly diminished in HATI- compared to vehicle-treated animals (Fig. 4F–H). To determine if diminished lesional Colla1 expression was due to promoter deacetylation in HATI-treated animals, we evaluated the *Colla1* promoter in the lesions by ChIP using anti-acetylH3. Diminished *Colla1* promoter acetylation was evident in lesions from HATI compared to vehicle-treated animals (Fig. 4I). Pharmacologically targeting Klf11/Sin3a/Hdac signaling by an epigenetic HATI thus significantly alleviated disease-associated fibrosis.

To test the translational specificity of Klf11/Sin3/Hdac-mediated Colla1 repression, Klf11^{-/-} animals with autologously induced endometriosis were treated with the reciprocal inhibitor (HDACI). In contrast to HATI, the extent of fibrosis remained unchanged in these HDACI-treated animals compared to those treated with vehicle (Supplemental Fig. S3). HDAC inhibition was thus ineffective on Colla1 expression

and fibrosis in Klf11^{-/-} animals, wherein this regulatory mechanism is absent. Taken together, these findings suggest that loss of repression of Colla1 by Klf11 correlated phenotypically with fibrosis and disease progression in the mouse model, which was reversed via targeted inhibitor therapy.

HDACI Treatment in wt Mice Augmented Fibrotic Progression

In contrast to Klf11^{-/-} mice, the Klf11/Sin3/Hdac regulatory pathway in wt animals is functional, resulting in Colla1 repression. These animals have low Colla1 expression levels and exhibit lesion regression. Hdac inhibition causes selective loss of deacetylation (mediated by Klf11/Sin3/Hdac), enabling persistent promoter acetylation and activated gene expression. Endometriosis lesions were surgically induced by suturing autologous uterine segments to parietal peritoneum in wt animals followed by SAHA (i.e., an HDACI) or control vehicle (DMSO) treatment. Wt animals treated with DMSO displayed lesion regression and minimal perilesional adhesions as expected (Fig. 5A, arrow). Fibrosis did not involve other abdominal viscera such as the mesentery and intestines (Fig. 5B, arrows). In contrast, Colla1 activation in HDACI-treated wt animals manifested as dense fibrosis extending from the lesion to other abdominal organs with loss of anatomic planes (Fig. 5, C white arrows, and D yellow arrow). Fibrosis involved the mesentery resulting in relative shortening of intestinal length and puckering (Fig. 5D, arrows). Wt animals treated with HDACI consequently had significantly increased disease progression scores compared to those treated with vehicle (Fig. 5E).

Lesional Colla1 mRNA and protein expression were increased in HDACI-treated animals and corresponded with fibrotic disease progression (Fig. 5F–H). To determine if increased lesional Colla1 expression from HDACI treatment was due to promoter hyperacetylation in treated wt animals, we evaluated the *Colla1* promoter in the lesions by ChIP using anti-acetylH3. *Colla1* promoter hyperacetylation was evident in lesions from HDACI-treated wt animals compared to those treated with vehicle (Fig. 5I). As with HATI, HDACI-treated animals also did not display any signs of drug toxicity and their weight remained unchanged throughout the study (Supplemental Fig. S2).

The translational specificity of Klf11/Sin3/Hdac-mediated Colla1 repression was further evaluated in wt autologous surgical models by treatment with the reciprocal inhibitor (HATI). In contrast to HDACI, fibrosis was minimal and unchanged compared to vehicle (Supplemental Fig. S4). HAT inhibition in wt animals was therefore ineffective because Klf11/Sin3/Hdac-mediated Colla1 repression is operative in these animals. Fibrosis and scarring in wt animals was thus specifically increased by HDACI but not by a reciprocal HATI via Colla1 activation. These findings corroborate the role and specificity of dysregulated Colla1 expression on fibrotic progression.

Diminished Lesional KLF11 Expression in Human Endometriosis Is Associated with Fibrosis

We previously showed that KLF11 expression is selectively diminished in endometriosis lesions compared to uterine endometrium [16]. KLF11 repressed COL1A1 via an epigenetic SIN3A/HDAC-mediated mechanism. Loss of Klf11/Sin3a/Hdac regulation resulted in prolific fibrosis in the animal model that was significantly ameliorated by targeted therapy.

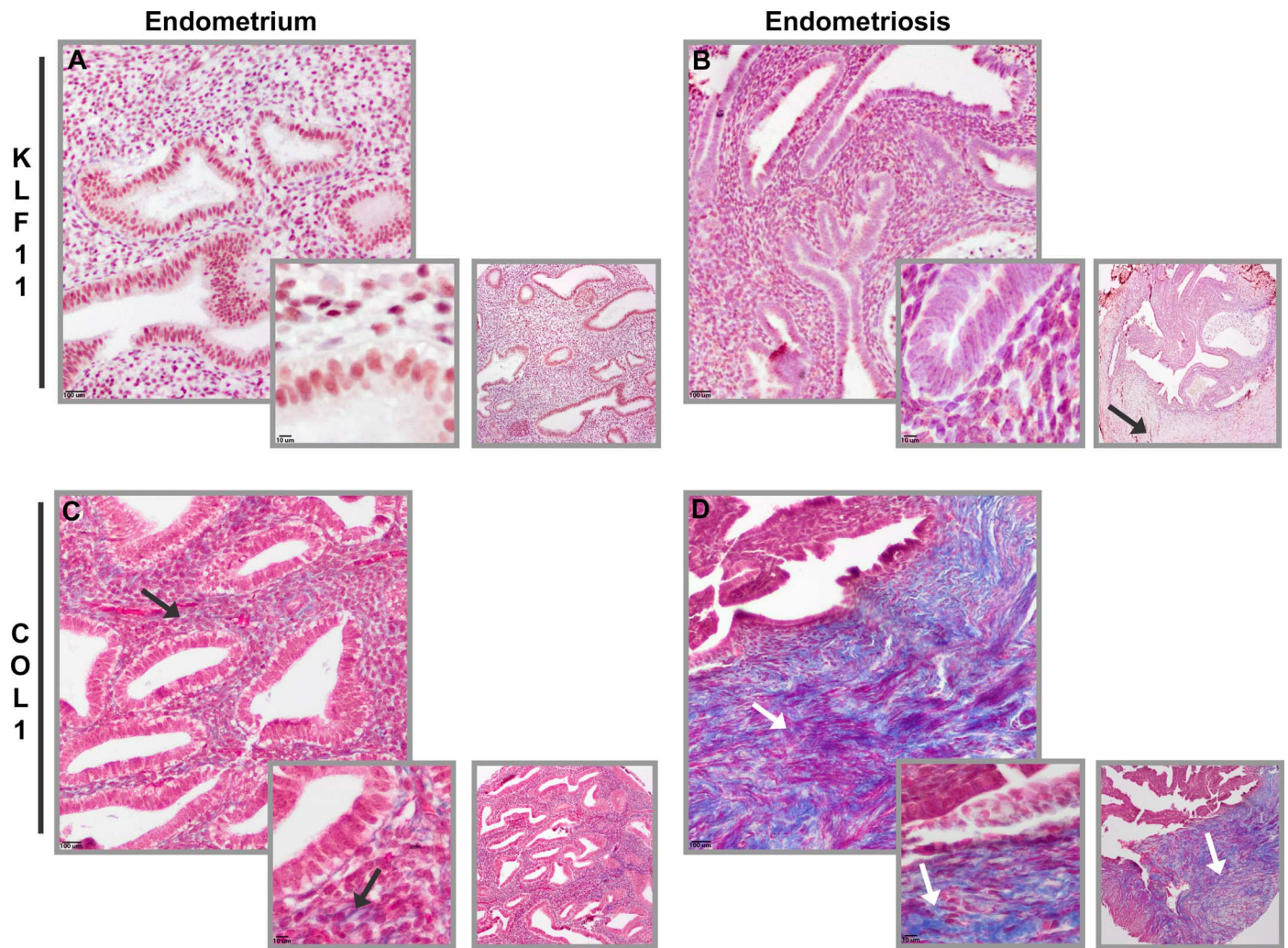


FIG. 6. Diminished lesional KLF11 expression in human endometriosis is associated with perilesional fibrosis. **A, B** KLF11 is expressed in endometrial epithelial and stromal nuclei. As previously observed, compared to uterine endometrium (**A**), KLF11 expression levels are diminished in endometriosis lesions (**B**). Perilesional collagen deposition is shown (**B**: side panel, black arrow). **C, D** COL1 expression was evaluated by Masson trichrome staining. In contrast to the KLF11 expression pattern, compared to uterine endometrium (**C**), COL1 levels were significantly up-regulated in endometriosis lesions and perilesional tissue (**D**); Masson trichrome staining shown for COL1 (Blue stain and arrows) ($n = 28$ matched samples). Magnification (**A–D**) $\times 100$ (main panel), $\times 400$ (inset), and $\times 20$ (side panel); bar = $100\ \mu\text{m}$ (main) and $10\ \mu\text{m}$ (inset).

To determine human disease relevance of this regulatory mechanism, we evaluated KLF11 and COL1 expression in human uterine endometrium and endometriosis lesions. Concordant with our previous findings, KLF11 expression levels were diminished in ectopically located endometriosis lesions compared to eutopic uterine endometrium (Fig. 6, A and B). In contrast, COL1 levels were significantly increased in perilesional tissues (Fig. 6, C and D). These lesions were associated with scarring. The animal model findings were thus concordant with both the in vitro characterized regulatory mechanism in T-HESCs and with corresponding gene expression levels in human disease, suggesting translational relevance.

DISCUSSION

Fibrosis is a ubiquitous disease mechanism that can affect body organs singly or systemically. Scarring from fibrosis replaces parenchyma and/or connective tissues to adversely affect functional capability and thereby resulting in disease. Despite its prominence as a key pathological mechanism, fibrosis has remained largely refractory to current medical and

surgical treatments. Endometriosis consists of displaced and ectopically located implants of uterine endometrial mucosa. The disease is often associated with other connective tissue disorders and progresses similarly with prominent fibrosis. We have used an endometriosis animal model to investigate disease-relevant fibrotic progression and determined the efficacy of novel targeted therapeutic approaches to treating it.

Progressive fibrosis and scarring was associated with lesion-specific diminished Klf11 expression (Fig. 1). KLF11 recruited the SIN3A/HDAC corepressor to the *COL1A1* promoter, resulting in histone deacetylation and gene repression (Figs. 2 and 3). This regulatory relationship was pharmacologically replicated by administration of a HATI to fibrosis-prone Klf11^{-/-} animals. Net promoter deacetylation from HATI therapy repressed Colla1 in the lesions with amelioration of scarring (Figs. 4 and 7B). In wt animals, the Klf11/Sin3a/Hdac mechanism represses Colla1 expression, and lesions typically regress with minimal residual fibrosis. To pharmacologically antagonize KLF11/Sin3a/Hdac, wt animals were administered an HDACI. As a result, the Colla1 promoter was hyperacetylated in the lesions, resulting in activated gene expression

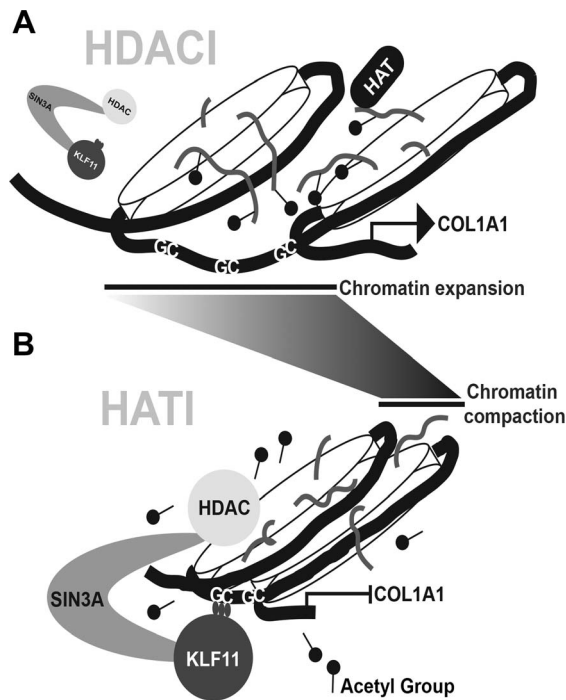


FIG. 7. Epigenetic histone deacetylase and acetyl transferase inhibitors alter gene expression levels via specific posttranslational promoter histone modification. **A**) In the presence of histone acetyl transferase (HAT), promoter histone tails (gray lines) are acetylated and the localized chromatin configuration is decondensed (expanded) to permit transcription (e.g., of COL1A1). This is physiologically replicated by loss of KLF11/SIN3A/HDAC binding and pharmacologically by HDACi therapy. **B**) In the presence of histone deacetylase (HDAC), promoter histone tails become deacetylated, resulting in chromatin compaction and transcriptional repression (e.g., of COL1A1). This is replicated physiologically by KLF11/SIN3A/HDAC binding to the COL1A1 promoter and pharmacologically by HATi therapy.

and appearance of de novo progressive fibrotic scarring (Figs. 5 and 7A). KLF11 and COL1 expression in human endometriosis lesions was concordant with and corroborated the animal model phenotype (Fig. 6, A–D). These findings indicate translational potential for targeting COL1A1/Coll1a1 expression through novel application of epigenetic inhibitors in chronic fibrotic diseases (Fig. 7).

KLF11 levels in endometriosis are diminished in a lesion-specific manner, although the mechanism is not known. In leiomyomas, KLF11 is diminished due to promoter methylation, a mechanism that may also be operative in endometriosis. We show here that epigenetic dysregulation is a significant adverse consequence of diminished KLF11 expression. Amelioration of abnormal gene expression as with mutations entails normoallelic replacement, which in uterine cells is technically, although not safely or ethically, feasible [27–31]. Coll1a1 activation from diminished Klf11 regulation can however be functionally overcome with selective epigenetic inhibitors, obviating the need for gene therapy. Epigenetic mechanisms are potentially reversible and successfully targeted by novel medications with increasing specificity [32–34]. These agents have been successful in early phase and clinical trials, which presages rapid translation of this work to human disease [35–38]. Other groups have shown that human endometriosis cells are responsive to epigenetic inhibitors [39].

KLF11 also recruits the HP1/histone methyl transferase (HMT) corepressor, which significantly has a role in liver fibrosis (Fig. 2A) [40]. We focused on HAT/HDAC-mediated

epigenetic regulation because inhibitors of these pathways are available, safe, and effective in early clinical trials. Given the heterogeneity of endometriosis, it is likely that other signaling pathways and epigenetic mechanisms such as HP1/HMT are selectively or cooperatively recruited in disease pathogenesis and remain our focus for further translational investigation [41–51]. Epigenetic inhibitors have also been evaluated in multisystem fibrosis trials with variable success, although none have focused on scar tissue collagen dysregulation or amelioration thereof [52–56].

In humans, endometriosis is most likely caused by intra-abdominal menstrual reflux through the fallopian tubes. The current animal endometriosis model is well characterized by several groups and has been invaluable in endometriosis research [57–61]. However, mice have a species-related limitation of not developing endometriosis spontaneously, likely from lack of physiological menstruation. This limitation of the mouse endometriosis model actually supports and extends the scope of our findings on the etiological role of increased Col1a1 expression in progressive fibrosis as well its pharmacological modulation. The natural history of fibrotic progression associated with surgically implanted peritoneal lesions is thus a robust model applicable to a wide spectrum of chronic, difficult to treat fibrotic diseases. Selection of the animal model enabled mechanistic investigation of the role of Klf11, a human disease-relevant gene as well as associated translationally relevant epigenetic mechanisms.

We used early generation HDAC and HAT inhibitors to establish the role of histone acetylation/deacetylation in disease pathogenesis and targeted therapy. Because they have been safely used in animals and in human clinical trials and therefore expect to rapidly translate these findings to the clinical setting [38, 52, 56, 62–64]. Although effective in these studies, these agents remain nonselective and could potentially broadly and adversely impact a subject's physiology. Ongoing development of newer generations of increasingly selective epigenetic inhibitors is expected to address these limitations and facilitate their novel application to a wide spectrum of disease. Discovery of novel epigenetic mechanisms and their inhibitors along with optimization of dose and delivery will thus significantly expand the scope and therapeutic capability in chronic disease.

REFERENCES

1. Bataller R, Brenner DA. Liver fibrosis. *J Clin Invest* 2005; 115:209–218.
2. Baumgart DC, Sandborn WJ. Crohn's disease. *Lancet* 2012; 380: 1590–1605.
3. Gross TJ, Hunninghake GW. Idiopathic pulmonary fibrosis. *N Engl J Med* 2001; 345:517–525.
4. Gabrielli A, Avvedimento EV, Krieg T. Scleroderma. *N Engl J Med* 2009; 360:1989–2003.
5. Hellebrekers BW, Kooistra T. Pathogenesis of postoperative adhesion formation. *Br J Surg* 2011; 98:1503–1516.
6. Thiery JP, Acloque H, Huang RY, Nieto MA. Epithelial-mesenchymal transitions in development and disease. *Cell* 2009; 139:871–890.
7. Keltz MD, Olive DL. Diagnostic and therapeutic options in endometriosis. *Hosp Pract* 1993; 28:15–16.
8. Giudice LC, Kao LC. Endometriosis. *Lancet* 2004; 364:1789–1799.
9. Revised American Fertility Society classification of endometriosis: 1985. *Fertil Steril* 1985; 43:351–352.
10. Vercellini P, Crosignani PG, Abbiati A, Somigliana E, Vigano P, Fedele L. The effect of surgery for symptomatic endometriosis: the other side of the story. *Hum Reprod Update* 2009; 15:177–188.
11. Nunes FR, Ferreira JM, Bahamondes L. Prevalence of fibromyalgia and quality of life in women with and without endometriosis. *Gynecol Endocrinol* 2014; 30:307–310.
12. Pasoto SG, Abrao MS, Viana VS, Bueno C, Leon EP, Bonfa E. Endometriosis and systemic lupus erythematosus: a comparative evaluation.

- tion of clinical manifestations and serological autoimmune phenomena. *Am J Reprod Immunol* 2005; 53:85–93.
13. Bieker JJ. Kruppel-like factors: three fingers in many pies. *J Biol Chem* 2001; 276:34355–34358.
 14. Bonnefond A, Lomber G, Buttar N, Busiah K, Vaillant E, Lobben S, Yengo L, Dechaume A, Mignot B, Simon A, Scharfmann R, Neve B, et al. Disruption of a novel Kruppel-like transcription factor p300-regulated pathway for insulin biosynthesis revealed by studies of the c.-331 INS mutation found in neonatal diabetes mellitus. *J Biol Chem* 2011; 286: 28414–28424.
 15. Yin P, Lin Z, Reierstad S, Wu J, Ishikawa H, Marsh EE, Innes J, Cheng Y, Pearson K, Coon JS V, Kim JJ, Chakravarti D, Bulun SE. Transcription factor KLF11 integrates progesterone receptor signaling and proliferation in uterine leiomyoma cells. *Cancer Res* 2010; 70:1722–1730.
 16. Daftary GS, Zheng Y, Tabbaa ZM, Schoolmeester JK, Gada RP, Grzenda AL, Mathison AJ, Keeney GL, Lomber GA, Urrutia RA. Novel role of the Sp/KLF transcription factor KLF11 in arresting progression of endometriosis. *PLoS One* 2013; 8:e60165.
 17. Ghosh AK. Factors involved in the regulation of type I collagen gene expression: implication in fibrosis. *Exp Biol Med* 2002; 227:301–314.
 18. Krikun G, Mor G, Alvero A, Guller S, Schatz F, Sapi E, Rahman M, Caze R, Qumsiyeh M, Lockwood CJ. A novel immortalized human endometrial stromal cell line with normal progestational response. *Endocrinology* 2004; 145:2291–2296.
 19. Zheng Y, Tabbaa ZM, Khan Z, Schoolmeester JK, El-Nashar S, Famuyide A, Keeney GL, Daftary GS. Epigenetic regulation of uterine biology by transcription factor KLF11 via posttranslational histone deacetylation of cytochrome p450 metabolic enzymes. *Endocrinology* 2014; 155: 4507–4520.
 20. Tabbaa ZM, Zheng Y, Daftary GS. KLF11 epigenetically regulates glycodelin-A, a marker of endometrial biology via histone-modifying chromatin mechanisms. *Reprod Sci* 2014; 21:319–328.
 21. Daftary GS, Lomber GA, Buttar NS, Allen TW, Grzenda A, Zhang J, Zheng Y, Mathison AJ, Gada RP, Calvo E, Iovanna JL, Billadeau DD, et al. Detailed structural-functional analysis of the Kruppel-like factor 16 (KLF16) transcription factor reveals novel mechanisms for silencing Sp/ KLF sites involved in metabolism and endocrinology. *J Biol Chem* 2012; 287:7010–7025.
 22. Suga H, Teraoka S, Ota K, Komemushi S, Furutani S, Yamauchi S, Margolin S. Preventive effect of pirfenidone against experimental sclerosing peritonitis in rats. *Exp Toxicol Pathol* 1995; 47:287–291.
 23. Lomber G, Mathison AJ, Grzenda A, Seo S, Demars CJ, Rizvi S, Bonilla-Velez J, Calvo E, Fernandez-Zapico ME, Iovanna J, Buttar NS, Urrutia R. Sequence-specific recruitment of heterochromatin protein 1 via interaction with Kruppel-like factor 11, a human transcription factor involved in tumor suppression and metabolic diseases. *J Biol Chem* 2012; 13:13026–13039.
 24. Lomber G, Bensi D, Fernandez-Zapico ME, Urrutia R. Evidence for the existence of an HP1-mediated subcode within the histone code. *Nat Cell Biol* 2006; 8:407–415.
 25. Zhang JS, Moncrieffe MC, Kaczynski J, Ellenrieder V, Prendergast FG, Urrutia R. A conserved alpha-helical motif mediates the interaction of Sp1-like transcriptional repressors with the corepressor mSin3A. *Mol Cell Biol* 2001; 21:5041–5049.
 26. Grzenda A, Lomber G, Zhang JS, Urrutia R. Sin3: master scaffold and transcriptional corepressor. *Biochim Biophys Acta* 2009; 1789:443–450.
 27. Daftary GS, Taylor HS. Efficient liposome-mediated gene transfection and expression in the intact human uterus. *Human Gene Therapy* 2001; 12: 2121–2127.
 28. Crystal RG. Transfer of genes to humans: early lessons and obstacles to success. *Science* 1995; 270:404–410.
 29. Lehrman S. Virus treatment questioned after gene therapy death. *Nature* 1999; 401:517–518.
 30. Marshall E. Gene therapy death prompts review of adenovirus vector. *Science* 1999; 286:2244–2245.
 31. Waddington SN, Kramer MG, Hernandez-Alcoceba R, Buckley SM, Themis M, Coutelle C, Prieto J. In utero gene therapy: current challenges and perspectives. *Mol Ther* 2005; 11:661–676.
 32. Fillmore CM, Xu C, Desai PT, Berry JM, Rowbotham SP, Lin YJ, Zhang H, Marquez VE, Hammerman PS, Wong KK, Kim CF. EZH2 inhibition sensitizes BRG1 and EGFR mutant lung tumours to TopoII inhibitors. *Nature* 2015; 520:239–242.
 33. Tang Y, Gholamin S, Schubert S, Willardson MI, Lee A, Bandopadhyay P, Berghold G, Masoud S, Nguyen B, Vue N, Balansay B, Yu F, et al. Epigenetic targeting of Hedgehog pathway transcriptional output through BET bromodomain inhibition. *Nat Med* 2014; 20:732–740.
 34. Ntziachristos P, Tsigirgos A, Welstead GG, Trimarchi T, Bakogianni S, Xu L, Loizou E, Holmfeldt L, Strikoudis A, King B, Mullenders J, Becksfort J, et al. Contrasting roles of histone 3 lysine 27 demethylases in acute lymphoblastic leukaemia. *Nature* 2014; 514:513–517.
 35. Yeo W, Chung HC, Chan SL, Wang LZ, Lim R, Picus J, Boyer M, Mo FK, Koh J, Rha SY, Hui EP, Jeung HC, et al. Epigenetic therapy using belinostat for patients with unresectable hepatocellular carcinoma: a multicenter phase I/II study with biomarker and pharmacokinetic analysis of tumors from patients in the Mayo Phase II Consortium and the Cancer Therapeutics Research Group. *J Clin Oncol* 2012; 30:3361–3367.
 36. Appleton K, Mackay HJ, Judson I, Plumb JA, McCormick C, Strathdee G, Lee C, Barrett S, Reade S, Jadavil D, Tang A, Bellenger K, et al. Phase I and pharmacodynamic trial of the DNA methyltransferase inhibitor decitabine and carboplatin in solid tumors. *J Clin Oncol* 2007; 25: 4603–4609.
 37. Chu QS, Sangha R, Spratlin J, J Vos L, Mackey JR, McEwan AJ, Venner P, Michelakis ED. A phase I open-labeled, single-arm, dose-escalation, study of dichloroacetate (DCA) in patients with advanced solid tumors. *Invest New Drugs* 2015; 33:603–610.
 38. Chu QS, Nielsen TO, Alcindor T, Gupta A, Endo M, Goytain A, Xu H, Verma S, Tozer R, Knowling M, Bramwell VB, Powers J, et al. A phase II study of SB939, a novel pan-histone deacetylase inhibitor, in patients with translocation-associated recurrent/metastatic sarcomas-NCIC-CTG IND 2007. *Ann Oncol* 2015; 26:973–981.
 39. Imesch P, Fink D, Fedier A. Romidepsin reduces histone deacetylase activity, induces acetylation of histones, inhibits proliferation, and activates apoptosis in immortalized epithelial endometriotic cells. *Fertil Steril* 2010; 94:2838–2842.
 40. Mathison A, Grzenda A, Lomber G, Velez G, Buttar N, Tietz P, Hendrickson H, Liebl A, Xiong YY, Gores G, Fernandez-Zapico M, Larusso NF, et al. Role for Kruppel-like transcription factor 11 in mesenchymal cell function and fibrosis. *PLoS One* 2013; 8:e75311.
 41. Han SJ, Hawkins SM, Begum K, Jung SY, Kovanci E, Qin J, Lydon JP, DeMayo FJ, O'Malley BW. A new isoform of steroid receptor coactivator-1 is crucial for pathogenic progression of endometriosis. *Nat Med* 2012; 18:1102–1111.
 42. Rogers PA, D'Hooghe TM, Fazleabas A, Giudice LC, Montgomery GW, Petraglia F, Taylor RN. Defining future directions for endometriosis research: workshop report from the 2011 world congress of endometriosis in Montpellier, France. *Reprod Sci* 2013; 20:483–499.
 43. Matsuzaki S, Darcha C. Involvement of the Wnt/ β -catenin signaling pathway in the cellular and molecular mechanisms of fibrosis in endometriosis. *PLoS One* 2013; 8:e76808.
 44. Bulun SE, Monsavaiz D, Pavone ME, Dyson M, Xue Q, Attar E, Tokunaga H, Su EJ. Role of estrogen receptor-beta in endometriosis. *Semin Reprod Med* 2012; 30:39–45.
 45. Zhao Y, Gong P, Chen Y, Nwachukwu JC, Srinivasan S, Ko C, Bagchi MK, Taylor RN, Korach KS, Nettles KW, Katzenellenbogen JA, Katzenellenbogen BS. Dual suppression of estrogenic and inflammatory activities for targeting of endometriosis. *Sci Transl Med* 2015; 7:271–279.
 46. McLaren J, Prentice A, Charnock-Jones DS, Millican SA, Müller KH, Sharkey AM, Smith SK. Vascular endothelial growth factor is produced by peritoneal fluid macrophages in endometriosis and is regulated by ovarian steroids. *J Clin Invest* 1996; 98:482–489.
 47. Lessey BA, Young SL. Integrins and other cell adhesion molecules in endometrium and endometriosis. *Semin Reprod Endocrinol* 1997; 15: 291–299.
 48. Miller MA, Meyer AS, Beste MT, Lasisi Z, Reddy S, Jeng KW, Chen CH, Han J, Isaacson K, Griffith LG, Lauffenburger DA. ADAM-10 and -17 regulate endometriotic cell migration via concerted ligand and receptor shedding feedback on kinase signaling. *Proc Natl Acad Sci U S A* 2013; 110:E2074–E2083.
 49. Berkley KJ, Dmitrieva N, Curtis KS, Papka RE. Innervation of ectopic endometrium in a rat model of endometriosis. *Proc Natl Acad Sci U S A* 2004; 101:11094–11098.
 50. Fung JN, Rogers PA, Montgomery GW. Identifying the biological basis of GWAS hits for endometriosis. *Biol Reprod* 2015; 92:87.
 51. Masuda H, Maruyama T, Gargett CE, Miyazaki K, Matsuzaki Y, Okano H, Tanaka M. Endometrial side population cells: potential adult stem/progenitor cells in endometrium. *Biol Reprod* 2015; 93:84.
 52. Levine MH, Wang Z, Bhatti TR, Wang Y, Aufhauser DD, McNeal S, Liu Y, Cheraghlu S, Han R, Wang L, Hancock WW. Class-specific histone/protein deacetylase inhibition protects against renal ischemia reperfusion injury and fibrosis formation. *Am J Transplant* 2015; 15:965–973.
 53. Ye Q, Li Y, Jiang H, Xiong J, Xu J, Qin H, Liu B. Prevention of pulmonary fibrosis via trichostatin A (TSA) in bleomycin induced rats. *Sarcoidosis Vasc Diffuse Lung Dis* 2014; 31:219–226.
 54. Williams SM, Golden-Mason L, Ferguson BS, Schuetz KB, Cavasin MA,

- Demos-Davies K, Yeager ME, Stenmark KR, McKinsey TA, Class I. HDACs regulate angiotensin II-dependent cardiac fibrosis via fibroblasts and circulating fibrocytes. *J Mol Cell Cardiol* 2014; 67:112–125.
55. Sunagawa Y, Morimoto T, Wada H, Takaya T, Katanasaka Y, Kawamura T, Yanagi S, Marui A, Sakata R, Shimatsu A, Kimura T, Takeya H, et al. A natural p300-specific histone acetyltransferase inhibitor, curcumin, in addition to angiotensin-converting enzyme inhibitor, exerts beneficial effects on left ventricular systolic function after myocardial infarction in rats. *Circ J* 2011; 75:2151–2159.
 56. Hutt DM, Herman D, Rodrigues AP, Noel S, Pilewski JM, Matteson J, Hoch B, Kellner W, Kelly JW, Schmidt A, Thomas PJ, Matsumura Y, et al. Reduced histone deacetylase 7 activity restores function to misfolded CFTR in cystic fibrosis. *Nat Chem Biol* 2010; 6:25–33.
 57. Cummings AM, Metcalf JL. Induction of endometriosis in mice: a new model sensitive to estrogen. *Reprod Toxicol* 1995; 9:233–238.
 58. Fortin M, Lepine M, Page M, Osteen K, Massie B, Hugo P, Steff AM. An improved mouse model for endometriosis allows noninvasive assessment of lesion implantation and development. *Fertil Steril* 2003; 80(Suppl 2): 832–838.
 59. Hirata T, Osuga Y, Yoshino O, Hirota Y, Harada M, Takemura Y, Morimoto C, Koga K, Yano T, Tsutsumi O, Taketani Y. Development of an experimental model of endometriosis using mice that ubiquitously express green fluorescent protein. *Hum Reprod* 2005; 20:2092–2096.
 60. Lee B, Du H, Taylor HS. Experimental murine endometriosis induces DNA methylation and altered gene expression in eutopic endometrium. *Biol Reprod* 2009; 80:79–85.
 61. Bruner-Tran KL, Eisenberg E, Yeaman GR, Anderson TA, McBean J, Osteen KG. Steroid and cytokine regulation of matrix metalloproteinase expression in endometriosis and the establishment of experimental endometriosis in nude mice. *J Clin Endocrinol Metab* 2002; 87: 4782–4791.
 62. Li HL, Liu C, de Couto G, Ouzounian M, Sun M, Wang AB, Huang Y, He CW, Shi Y, Chen X, Nghiem MP, Liu Y, et al. Curcumin prevents and reverses murine cardiac hypertrophy. *J Clin Invest* 2008; 118:879–893.
 63. Nural-Guvener HF, Zakharova L, Nimlos J, Popovic S, Mastroeni D, Gaballa MA. HDAC class I inhibitor, mocetinostat, reverses cardiac fibrosis in heart failure and diminishes CD90+ cardiac myofibroblast activation. *Fibrogenesis Tissue Repair* 2014; 7:10.
 64. Jaffe RC, Ferguson-Gottschall SD, Gao W, Beam C, Fazleabas AT. Histone deacetylase inhibition and progesterone act synergistically to stimulate baboon glycodefin gene expression. *J Mol Endocrinol* 2007; 38: 401–407.